The Astrophysical Journal, 651:704–712, 2006 November 10

DUST ABSORPTION ALONG THE LINE OF SIGHT FOR HIGH-REDSHIFT OBJECTS

M. Trenti and M. Stiavelli
Space Telescope Science Institute, 3700 San Martin Drive, Baltimore, MD 21218; trenti@stsci.edu, mstiavel@stsci.edu
Received 2006 January 31; accepted 2006 July 10

ABSTRACT

We estimate the optical depth distribution of dust present in absorption systems along the line of sight of high-redshift galaxies and the resulting reddening. We characterize the probability distribution of the transmission to a given redshift and the shape of the effective mean extinction law by means of analytical estimates and Monte Carlo simulations. We present our results in a format useful for applications to present samples of high-redshift galaxies and discuss the implications for observations with the *James Webb Space Telescope*. Our most realistic model takes into account the metallicity evolution of damped Lyα absorbers and predicts that the effects of dust absorption are modest: at redshift $z \gtrsim 5$ the transmission is above 0.8 at an emitted wavelength $\lambda_e = 0.14$ μm with probability 90%. Therefore, dust obscuration along the line of sight will affect only marginally observations at very high redshift.

Subject headings: dust, extinction — galaxies: high-redshift — galaxies: ISM — intergalactic medium

Online material: color figures

1. INTRODUCTION

Dust along the line of sight affects the observations of distant astronomical objects, and its effects on both extinction and reddening need to be taken into account. In the case of high-redshift quasars, this problem was initially addressed by Ostriker & Heisler (1984), and it has been the subject of several later investigations. Fall & Pei (1989, 1993) developed a comprehensive theoretical framework to quantify the effects of dust along the line of sight and characterize sample selection effects induced by damped Lyα (DLA) absorbers. The reddening measurements by Pei et al. (1991), based on a sample of 13 DLA systems with average absorption redshift $\langle z_{\rm abs} \rangle \approx 2.6$, evidenced a reddening of background quasars with DLA spectral fingerprints with respect to a control sample without intervening absorbers. The reddening was measured from the shift of the average slope of the quasar spectral energy distribution between the two samples, which was found to be $\langle \Delta\alpha \rangle = 0.5$ (significant at above the 99% confidence level).

Some recent determinations based on larger samples of quasars (Murphy & Liske 2004; Ellison et al. 2005) do not confirm the earlier conclusions by Pei et al. (1991), and the new limits set on the dust obscuration along the line of sight are down by 1 order of magnitude with respect to the earlier estimates. Murphy & Liske (2004) find that $\Delta\alpha \leq 0.2$ at 3 σ for a larger sample of absorbers at $\langle z_{\rm abs} \rangle \approx 3$. This implies a reddening $E(B-V) < 0.02$ mag (at 3 σ). Unfortunately, the determination of the dust absorption at high redshift is intrinsically an indirect measurement, and there is the possibility that the real dust content is higher than these lower estimates due to observational biases such as sample selection effects. Indeed, for a subsample of DLA absorbers selected by the presence of the Ca II absorption line, Wild & Hewett (2005) and Wild et al. (2006) find a significant evidence of reddening at moderate redshift [$\langle E(B-V) \rangle \gtrsim 0.1$ at $z_{\rm abs} \approx 1$]; similarly, York et al. (2006) measure $\langle E(B-V) \rangle$ up to 0.085 for Mg II absorbers at $z_{\rm abs} \approx 1.4$. Thus, any modeling of dust effects on high-redshift objects will need to take into account possible selection effects.

Surprisingly, very little consideration is generally given to the effects of dust obscuration along the line of sight for high-redshift, nonactive galaxies. Clearly, if the effects of dust absorption have been detected for quasars, it is likely that they will affect every other object at similar distances. Nonetheless, it is common practice in observations of high-redshift galaxies to consider the obscuration of dust as a screen localized at the emitter location (see, e.g., Papovich et al. 2001), adopting a description of the dust properties like that used for local starburst galaxies (Calzetti et al. 1994).

The primary goal of this paper is therefore to estimate the fraction of essentially unobscured lines of sight for very high-redshift objects ($z \lesssim 20$) and their average transmission. The estimation of this quantity is much more robust with respect to uncertainties and biases in the observed distribution of absorbers than the measure of the amount of dust in DLA systems (whose determination is outside the scope of this work). In fact, while a small number of optically thick absorbers, missed in magnitude-limited surveys, could in principle contain the majority of dust in the universe, their effect on the average transmission along a random line of sight would be limited by their covering factor. The CORALS radio-selected survey (Ellison et al. 2001) probes 66 lines of sight with complete optical follow-up detection. The probability of finding an optically thick absorber along a random line of sight is therefore below 4.9% at the 99% confidence level (and below 2.9% at the 95% confidence level).

In § 2 we present our model for the absorbers, which is calibrated in § 3 up to redshift $z \approx 5$ on the measurements from recent DLA surveys (Ellison et al. 2001; Prochaska et al. 2005). For extrapolation to higher redshift we assume an unevolving comoving density of DLA systems and a dust-to-gas ratio decreasing exponentially with redshift (§ 3.1). We also consider a wider set of input parameters to investigate different parameters extrapolation recipes and to study a higher dust content that could be missed due to selection effects. In § 4 we describe our Monte Carlo code, which allows us to characterize the full probability distribution of absorption that is presented in § 5. Section 6 sums up.

2. ABSORBER MODELING

Given a source at redshift z_e, we are interested in modeling the absorption due to dust residing in DLA systems (i.e., absorption systems with neutral hydrogen column density, N_d, above 2×10^{20} cm^{-2}). Our approach is inspired by the models of Møller & Jackobsen (1990) and Madau (1995) (see also Fall & Pei 1993), in which the absorber distribution is treated as an input parameter that we calibrate to observations in § 3.

We assume a discrete probability distribution of absorbers along the line of sight up to redshift z_e with a *separable* probability distribution in column density (N_d) and redshift (z). This probability distribution is further assumed to be Poissonian per unit redshift, so that

$$p(N_d, z) = \phi(N_d)\psi(z), \tag{1}$$

with $E[d\psi(z)/dz] = n(z)$ (in this paper the symbol $E_p[f]$ means the expectation value of f under the probability measure p, and we drop the subscript p if it is clear what probability measure we are referring to).

We consider the following forms for the column density distribution $\phi(N_d)$: (1) a gamma function, the best-fitting functional form observationally, identified by Prochaska et al. (2005),

$$\phi(N_d) \propto \left(\frac{N_d}{N_\gamma}\right)^{-\alpha_1} \exp\left(-\frac{N_d}{N_\gamma}\right), \tag{2}$$

where N_d is in $[N_{\rm min}; +\infty]$ and (2) a power law (computationally friendlier in our Monte Carlo approach due to the simple analytical primitive) in a range $[N_{\rm min}, N_{\rm max}]$,

$$\phi(N_d) \propto (N_d)^{-\alpha_2}. \tag{3}$$

The normalization for the function $\phi(N_d)$ is chosen so as to have $\int dN_d\, \Phi(N_d) = 1$.

The average number of absorbers per unit redshift $n(z)$ is assumed to vary as

$$n(z) = A\frac{dX}{dz}, \tag{4}$$

where

$$\frac{dX}{dz} = \frac{H_0}{H(z)}(1+z)^2 = \frac{(1+z)^2}{\sqrt{\Omega_\Lambda + \Omega_M(1+z)^3}}. \tag{5}$$

Here, we adopt a *Wilkinson Microwave Anisotropy Probe* (*WMAP*) concordance cosmology with $\Omega_\Lambda = 0.7$, $\Omega_M = 0.3$, and $H_0 = 70$ km s^{-1} Mpc^{-1} (Spergel et al. 2006).

The absorption cross section of dust located at z_a is assumed to be $\sigma(\lambda_a)$ in its rest frame. For an observed wavelength λ_o this can be written as $\sigma(\lambda_o/(1+z_a))$. In the B band in the absorber rest frame, $\lambda_a = 0.44$ μm, we assume that the optical depth of the dust can be written as

$$\tau_B = N_d\sigma(0.44\ \mu{\rm m}) = k\frac{N_d}{10^{21}\ {\rm cm}^{-2}}, \tag{6}$$

where k is a dimensionless dust-to-gas ratio parameter (k is of order unity for the Milky Way).

At different wavelengths the absorption cross section can be expressed via an extinction curve $\xi(\lambda)$,

$$\xi(\lambda) = \frac{\sigma(\lambda)}{\sigma(\lambda_B)}. \tag{7}$$

Thus, for a single cloud at redshift z_a we can write the optical depth $\tau(\lambda_o)$ as

$$\tau(\lambda_o) = \frac{kN_d}{10^{21}\ {\rm cm}^{-2}}\xi(\lambda_o/(1+z_a)). \tag{8}$$

Given these assumptions, we can compute analytically, down to the numerical evaluation of a single integral over redshift, the average value for the transmission coefficient $q(\lambda_o, z_e) = \exp[-\tau(\lambda_o, z_e)]$ to a source at redshift z_e. The computation is straightforward (see Appendix A in Møller & Jackobsen 1990) and yields

$$E[q(\lambda_o, z_e)] = \exp\left(-\int_0^{z_e} dz\, n(z)\{1 - E_\phi[q(\lambda_o, z)]\}\right), \tag{9}$$

where

$$q(\lambda_o, z) = \exp\left[-k(z)N_d\xi\left(\frac{\lambda_o}{1+z}\right)\right]. \tag{10}$$

We recall that $E_\phi[f]$ denotes the expectation value of f under the probability distribution ϕ.

From the average value of the transmission coefficient, we can define an *effective* optical depth,

$$\tau^{(\rm eff)} = -\log E[q(\lambda_o, z_e)]. \tag{11}$$

This quantity is a measure of the average departure from unit transmission and is more physically relevant than the mean optical depth for the purpose of characterizing the fraction of obscured lines of sight in the sky (see also Madau 1995). In fact, the mean value of the optical depth is very sensitive to the detailed properties of the high tail in the τ distribution. The concept can be easily illustrated with the following example. Consider 100 lines of sight, one of which with a really optically thick absorber ($\tau = 10^4$), while the others are optically transparent. In this case, the *effective* optical depth (eq. [11]) is $\tau^{(\rm eff)} \approx 0.01$ and correctly captures the fact that with probability 1%, a line of sight is optically thick. The average optical depth is instead $E[\tau] = 10$, a very misleading value if applied to the estimation of the probability of having a line of sight free from absorption.

3. PARAMETER ESTIMATION FROM DLA DATA

We can take advantage of recent surveys (Ellison et al. 2001; Prochaska et al. 2005; Akerman et al. 2005; Rao et al. 2006) that have measured the observed redshift column density distribution and metallicity for DLA systems to critically examine the assumptions adopted in our model and to estimate its free parameters.

In principle, the calibration of our model for the absorbers appears straightforward, as it relies on the observed statistics of Lyα features in the spectra of several thousands of quasars over an extended redshift range. Unfortunately, for optically selected quasar samples the observed distribution of DLA systems is in general a biased estimator of the intrinsic distribution as highly obscured lines of sight are preferentially missed for an optically selected sample. However, as we are interested in characterizing the average transmission to high z, and not in the measure of the comoving gas density in DLA systems, the dust bias at the high end of the column density distribution of neutral gas is of limited impact. In fact, if a small fraction ϵ of optically thick absorbers is missed in a survey, this will only introduce a relative error of order ϵ in the average transmission. On the other hand, The comoving gas density may be affected by an arbitrarily large error if these missed absorbers dominate the gas density budget.

For the calibration we resort to two samples of DLA data. The first is the radio-selected CORALS survey (Ellison et al. 2001), which has the advantage of being free from dust bias but

TABLE 1
ADOPTED PARAMETERS

ID	A	α_2	$N_{\rm min}$	$N_{\rm max}$	α_κ
Pr05_Γ[a]	0.0715	1.8	0.2	∞	1
Pr05_P	0.0715	2.2	0.2	10	1
El01_a	0.0910	2.1	0.2	10	1
El01_b	0.0910	2.1	0.2	10	0.5
El01_c	0.0910	2.1	0.2	10	0.75
El01_d	0.0910	2.1	0.2	20	1
El01_e	0.0910	2.1	0.2	100	1
El01_f	0.0910	2.1	0.2	10	$\theta(7-z)$
El01_g	0.0910	2.1	0.2	10	1+"DLAbricks"
El01_h	0.0910	2.1	0.2	10	1+"disks"

NOTE.—Summary table with the parameters used to compute dust absorption.
[a] For model Pr05_Γ $N_\gamma = 3.03$, and the value in the α column is for α_1 instead of α_2.

consists of only 66 quasars with detection of 19 intervening DLA systems. The statistical uncertainties in the values of the estimated parameters are rather large (reported as entries "El01" in Table 1). We therefore also consider the significantly larger, but optically selected, Sloan Digital Sky Survey, Data Release 3 (SDSS DR3) DLA data set (Prochaska et al. 2005), which consists of 525 DLA systems identified in the spectra of 4568 quasars with signal-to-noise ratio above 4. This data set, while providing an excellent statistical accuracy (the *observed* neutral gas density in DLA systems is measured with relative error below 10%; see Prochaska et al. 2005), may be affected by systematic uncertainties for the high column density tail of the DLA system distribution (see Trenti & Stiavelli [2006] for a characterization of the systematic errors in the SDSS DR3 DLA data set). The sets of parameters estimated using these data are reported as entries "Pr05" (SDSS) in Table 1.

The absorber column density distribution $\Phi(N_d)$ has been characterized starting from the empirical distributions for the CORAL and SDSS surveys using a maximum likelihood estimator and plotting, in Figure 1, the likelihood function.

We estimate the values for the parameters in the gamma function description for $\phi(N_d)$ using only the SDSS data, as the fit would have too many free parameters for the size of the CORALS survey. With our analysis we rederive the same parameters identified by Prochaska et al. (2005) (entry "Pro05_Γ" in Table 1). Namely, we assume the standard DLA limit $N_{\rm min} = 2 \times 10^{20}$ cm^{-2}, and we find $\alpha_1 = 1.8$ and $N_\gamma = 3 \times 10^{22}$ cm^{-2}. For the single power-law description we obtain $\alpha_2 = 2.2$ (SDSS) and $\alpha_2 = 2.1$ (CORALS), adopting $N_{\rm min} = 2 \times 10^{20}$ cm^{-2} (the standard DLA limit density) and $N_{\rm max} = 10^{22}$ cm^{-2}. This cutoff has been introduced with the goal of eliminating unphysical high-N_d tails in the distribution of gas column densities. The cutoff has been set to a value marginally higher than all the N_d measurements in the SDSS and CORALS survey. We also explore different power-law models with increasingly high value for the cutoff (models El01_a, El01_d, and El01_e) in order to assess the effects of a small additional number of optically missed absorbers with increasingly high column densities. While the SDSS data rule out a single power law at a confidence level above 3 σ for the observed column density distribution, this description may still be valid for the intrinsic distribution. Unfortunately, the CORALS data do not allow us to significantly constrain the functional form of $\phi(N_d)$ (see Ellison et al. 2001). The bias in an optically selected DLA survey maps an *intrinsic* power-law distribution of column densities into an *observed* gamma function distribution (Fall & Pei 1993).

In our approach, A is assumed to be independent of redshift, i.e., we are assuming a constant comoving number of absorbers. Because of the separability of equation (1), this implies a constant comoving density of neutral gas in DLA systems ($\Omega_{\rm H\,I}^{\rm (DLA)}$). The SDSS data (Prochaska et al. 2005) show evolution of $\Omega_{\rm H\,I}^{\rm (DLA)}$ by about a factor of 2, mainly in the redshift range [2.2, 3]. However, at lower redshift the measured gas density seems to be more in-line with the $z > 3$ values (see Fig. 22 in Prochaska et al. 2005 and Fig. 16 in Rao et al. 2006), so this schematic modeling appears to be in reasonable agreement with the observations. The combined evolution seen by Rao et al. (2006) in the line and column density distributions at approximately constant $\Omega_{\rm H\,I}^{\rm (DLA)}$ would

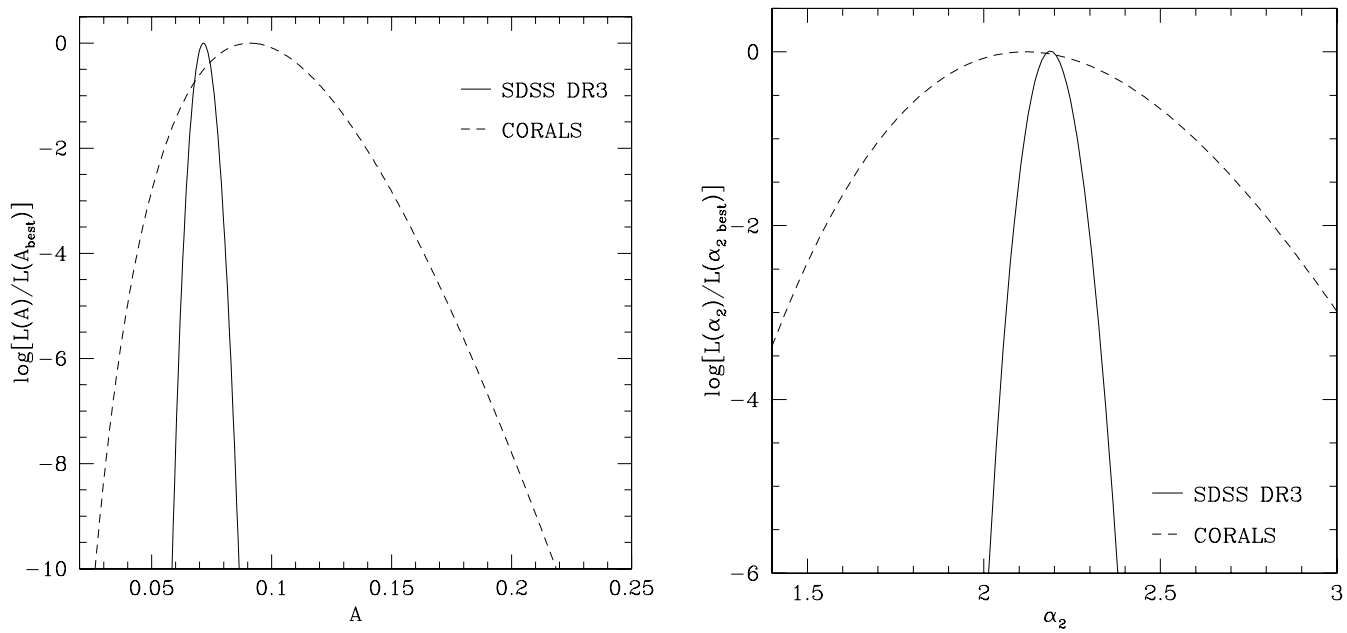

FIG. 1.—Maximum likelihood estimation for the parameters A (*left*) and α_2 (*right*), based on the data from Ellison et al. (2001; *dotted line*) and from Prochaska et al. (2005; *solid line*). For each data set we plot the likelihood L (log scale) of the parameters normalized to the maximum value.

affect the separability assumption of equation (1). This would complicate the numerical treatment of our model, but would not significantly change the value of the effective extinction to a given redshift, which, under the assumption of optically thin absorbers, depends in first approximation only on the comoving dust (i.e., neutral gas) density. The average transmission would depend more critically on the precise form of equation (1) if a significant population of optically thick absorbers is present, but this is an unlikely scenario given the complete optical follow-up detection in the radio-selected CORALS survey (Ellison et al. 2001).

In order to estimate A, we have tested the covering factor of DLA systems. Starting from the published data, we have identified for each quasar in the two samples the range of redshift in which the presence of DLA systems was detectable (from Table 1 in Prochaska et al. [2005] and from Table 3 in Ellison et al. [2001]), computed the expected number of DLA systems in that interval, and obtained A by evaluating the likelihood of getting the observed number distribution of DLA counts.

The maximum likelihood estimation for A given the two data sets is reported in Figure 1, the maximum value for CORALS is at $A = 0.0910$, while the maximum for SDSS is at $A = 0.0715$. Assuming the SDSS value for A, the CORALS data are marginally consistent; the higher CORALS result may be due to small number fluctuations at the 1 σ level (see the likelihood ratio in Fig. 1). An alternative possibility is that the discrepancy is due to an obscuration bias for SDSS. This is however highly unlikely, as the covering factor determination is dominated by DLA systems at the low end of the column density distribution, where the obscuration bias is negligible. The A value estimated from the SDSS data could even be an overestimate for the intrinsic A because of a Malmquist bias. That is, more absorbers with column density below the DLA limit have been scattered into the DLA sample than absorbers above the limit have been scattered out (T. O'Meara et al. 2006, in preparation; J. X. Prochaska 2006, private communication).

For these parameters we can compute the comoving density of neutral gas in DLA systems implied by our model (see, e.g., Prochaska et al. 2005),

$$\Omega_{\rm H\,I}^{\rm (DLA)} = \frac{\mu m_{\rm H} H_0}{c\rho_c} A E_\Phi[N_d], \tag{12}$$

where $m_{\rm H}$ is the mass of the hydrogen atom, $\mu = 1.3$ is a correction factor for the composition of the gas, c is the speed of light, and ρ_c is the critical density of the universe. We find $\Omega_{\rm H\,I}^{\rm (DLA)} = 0.81 \times 10^{-3}$ for SDSS data fitted to a gamma function, $\Omega_{\rm H\,I}^{\rm (DLA)} = 0.84 \times 10^{-3}$ for the SDSS data fitted to a power law, and $\Omega_{\rm H\,I}^{\rm (DLA)} = 1.17 \times 10^{-3}$ for CORALS data (with $A = 0.0910$). The agreement with the published value from SDSS is excellent [see Table 9 in Prochaska et al. 2005; their unbinned measurement is $(0.817 \pm 0.05) \times 10^{-3}$], though our data cannot be compared directly with the analysis in Ellison et al. (2001), as they have used a different cosmology ($\Omega_M = 1$ and $\Omega_\Lambda = 0$).

The value of the dust-to-gas ratio k for DLA systems depends on their metallicity Z, and as a first approximation, we can consider a linear dependence of the dust-to-gas ratio on Z. DLA systems are generally characterized by a low metallicity and by a moderate evolution of their properties with the redshift (Wolfe et al. 2005). Their metallicity has been measured in several surveys, and the average metallicity in optically and radio-selected samples appears consistent (Akerman et al. 2005). Here, we consider the compilation by Kulkarni et al. (2005) (see also Prochaska et al. 2003), and we approximate the reported measurements (Fig. 13 in Kulkarni et al. 2005) with a linear function for $\log[Z(z)]$, which provides a good agreement with the data in the redshift range $2 \lesssim z \lesssim 5$,

$$\frac{Z(z)}{Z_\odot} = 0.2 \times 10^{-0.2z}. \tag{13}$$

By considering a typical dust-to-gas ratio $k = 0.8$ for our galaxy ($Z \approx Z_\odot$ with $\approx$50% of the metals locked in dust grains), this translates into an observed dust to gas ratio of

$$k(z) = 0.16 \times 10^{-0.2z}. \tag{14}$$

To account for uncertainties in the measure of $Z(z)$ and for a smaller fraction of metals depleted into dust, we introduce a free factor α_κ for the intrinsic dust-to-gas ratio $k(z)$,

$$k(z) = \alpha_\kappa k_o(z). \tag{15}$$

Realistic values for α_κ range in the interval [0, 1]; $\alpha_\kappa = 0.5$ corresponds to 25% of the total metal amount in dust grains (see, e.g., Pettini et al. 1997; Prochaska & Wolfe 2002), while $\alpha_\kappa = 1$ implies a depletion factor like that in the Milky Way (Pei & Fall 1995; Pei et al. 1999). Our main results are presented in terms of $\alpha_\kappa = 1$, so that we effectively obtain upper limits on the obscuration along the line of sight. In § 5 we also discuss scenarios with $\alpha_\kappa < 1$.

The extinction curve $\xi(\lambda)$, in the absorber rest frame, is assumed to be as measured in and parameterized for the Small Magellanic Cloud (Pei 1992). In fact, extinction curves similar to those measured for our Galaxy and for the Large Magellanic Cloud seem to be ruled out by the current observational data (Ellison et al. 2005; York et al. 2006). Extinction curves for DLA systems at low redshift start to be directly measured and highlight a rather complex picture; Junkkarinen et al. (2004) have measured $\xi(\lambda)$ for a $z = 0.524$ DLA absorber, finding some similarities with the Galactic extinction curve. For our purposes the use of a different extinction curve would not affect our results significantly, as the redshift averaging process over many absorbers tends to smooth out the specific features of the input curve.

3.1. *Extrapolation of Parameters Up to $z \approx 20$*

As we are mainly interested in characterizing the expected absorption for future observations at $z > 6$, the parameters that have been tuned to the properties of DLA systems at $z \lesssim 5$ must be extrapolated into a redshift region with no observational constraints. Qualitatively, a monotonic metal (and dust) abundance appears plausible even before reionization, when all hydrogen is neutral. Indeed, as the redshift increases, the metallicity decreases, so one expects that the average local content of dust will progressively be reduced.

Our derivation of the average transmission depends on the comoving dust distribution, which we treat as the product of dust-to-gas ratio times neutral hydrogen distribution in discrete systems, which we identify as DLA systems at $z < 5$, but that could simply be the sites of metal production at higher z.

At a sufficiently large z the average comoving density of neutral gas will stay approximately constant; the star formation rate should drop after $z \approx 6$, and this, combined with progressively less time available for star formation, means that the initial reserve of gas should remain almost undepleted. Eventually, in a hierarchical formation scenario, one can expect that the neutral gas will reside in more numerous Lyα systems with smaller column densities, but this will influence only marginally the

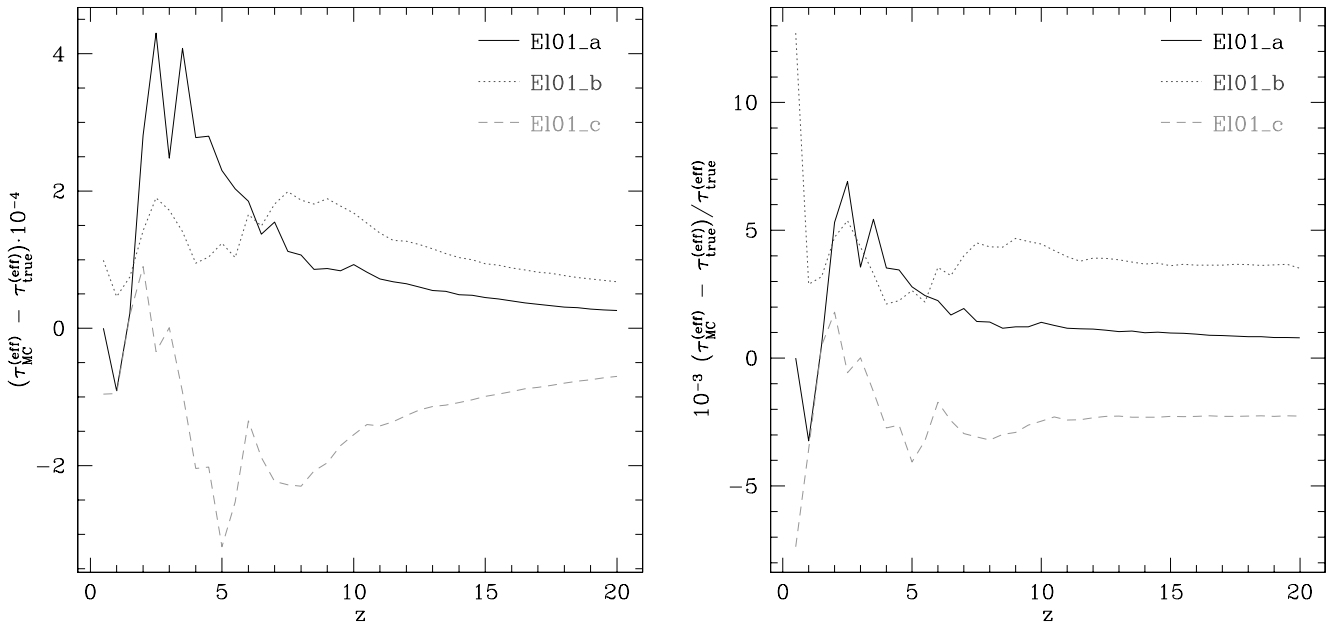

FIG. 2.— Absolute (*left*) and relative (*right*) error for the effective optical depth computed via our MC method using 4×10^5 random lines of sight and compared with the analytical value from eq. (9) for the models El01_a, El01_b, and El01_c. [*See the electronic edition of the Journal for a color version of this figure.*]

value of the expected absorption along the line of sight at constant comoving gas density. In fact, given their very low dust-to-gas ratio, these primordial absorbers are expected to be optically thin, so the average transmission will not depend in first approximation on the details of the distribution and will be proportional to the integrated comoving dust density.

These arguments led us to choose to extrapolate our set of parameters with minimal assumptions: constant A, i.e., constant comoving $\Omega_{\rm H\,I}$ density, and exponentially decreasing metallicity, as given by extension of our equation (14). These extrapolations are consistent with the asymptotic behavior of global models for the chemical evolution of DLA systems, like those developed by Pei & Fall (1995).

The use of equation (13) implies a metallicity of $1.2 \times 10^{-3}\ Z_\odot$ at $z = 11$, which is the redshift of reionization derived from the *WMAP* 3 yr Compton optical depth (Spergel et al. 2006). This value is comfortably larger than the minimum metallicity required for reionization (by Population III stars, $Z \approx 1.2 \times 10^{-4}\ Z_\odot$; Stiavelli et al. 2004). This extrapolation could thus be considered conservative.

An additional test can be performed in terms of the predictions given by models for the formation and chemical enrichment of DLA systems based on cosmological hydrodynamical simulations (Cen et al. 2003) or on semianalytical prescriptions (Johansson & Efstathiou 2006). These models confirm a relatively slow but progressive decrease of the metallicity, while they evidence a sharp drop in the comoving density of neutral gas in DLA systems at $z > 7$ (P. H. Johansson & G. Efstathiou 2006, private communication), which, however, could be due to the built-in assumptions, e.g., coeval evolution with equal ages.

To check what would be the consequences for our estimates in a scenario where the number of absorbers drops significantly at $z > 7$, we have run some Monte Carlo simulations assuming that there are no absorbers at $z > 7$ and compared the obscuration given by these models with that predicted by those with extrapolation at constant A. The results (presented in detail in § 5) evidence a modest variation in the average transmission. This is easily understood as, given the exponential decrease of k, the impact of $z > 7$ absorbers is limited.

4. OUR MONTE CARLO CODE

In order to compute the probability distribution for the optical depth, we resort to a Monte Carlo code. Our code accepts general input functions $\Phi(N_d)$, $n(z)$, $k(z)$, and $\xi(\lambda)$ and generates the chosen number of discrete realization for the DLA system distribution along lines of sight for a given emission redshift z_e. The cumulative probability distribution for the optical depth to redshift z_e is then built.

For each discrete realization, we begin by integrating up to z_e the redshift distribution of DLA systems $n(z)$, so as to obtain the expected total number of absorbers along the line of sight,

$$n_{\rm tot} = \int_0^{z_e} n(z)\, dz. \tag{16}$$

A Poisson random variable with mean $n_{\rm tot}$ representing the realized number of absorbers is generated using a standard subroutine from Press et al. (1992). The redshift for each absorber is then randomly assigned by inversion of the primitive of $n(z)$, evaluated numerically. Similarly, the column density for each absorber is assigned via random sampling by inversion of the primitive for $\Phi(N_d)$. Once the redshift and column density for each absorber has been assigned, the optical depth at the observed wavelength of interest is computed for each absorber via equation (8). The total optical depth is given by summing over all the absorbers along the line of sight.

The accuracy of the code is estimated by evaluating the variance for selected levels in the optical depth distribution (median, upper, and lower 1 and 2 σ points). In addition, the effective optical depth is compared to the analytical value from equation (9). The effective optical depth and the median are evaluated, at a fixed number of discrete realizations, with greater accuracy than the 1 and 2 σ points. Especially for the 2 σ contours, 1 order of magnitude more realizations are needed for an accuracy comparable to that reached for the effective optical depth. For our purposes we are satisfied with an absolute error below 10^{-3} for $\tau^{(\rm eff)}$. This is reached with about 10^5 random lines of sight. Depending on the redshift of emission (lines of sight for low z_e have an expected

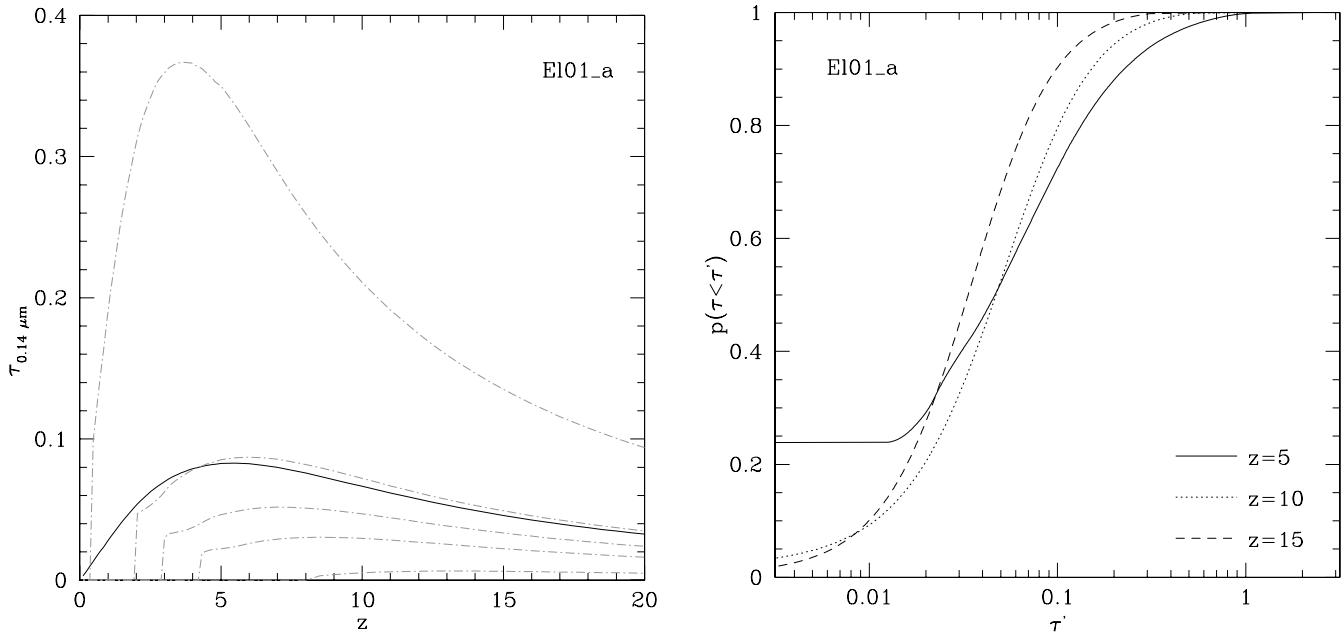

FIG. 3.—*Left:* Effective optical depth $\tau^{(\mathrm{eff})}$ as a function of redshift at $\lambda_e = 0.14$ μm (*solid line*) for the El01_a model. The dash-dotted lines represent, starting from the top in the left panel, the top 95% contour in the distribution of optical depth, the top 68%, the median, the bottom 32%, and the bottom 5%. *Right:* Cumulative probability distribution for the optical depth at $\lambda_e = 0.14$ μm along lines of sight to different redshifts (*solid line:* $z = 5$; *dotted line:* $z = 10$; *dashed line:* $z = 15$). The curves have been generated with a MC code using 4×10^5 random lines of sight. [*See the electronic edition of the Journal for a color version of this figure.*]

number of intervening DLA system much less than 1, so the relative variance in the Monte Carlo code is higher), this translates into a relative error below 10^{-2} at low z_e and of about $(2\text{–}3) \times 10^{-3}$ at high z_e for the Monte Carlo simulations presented in this paper (see Fig. 2).

5. RESULTS: ABSORPTION PROBABILITY DISTRIBUTION

In Figures 3–4 we plot the effective optical depth $\tau^{(\mathrm{eff})}$ (at the emitter rest frame $\lambda_e = 0.14$ μm) for a given redshift, obtained using our models El01_a and El01_b, which employ the best-fitting value for A from the CORALS survey (which represents a generous upper limit for A; see § 3), and $\alpha_\kappa = 1$ (50% of metals in dust) for model "a" and $\alpha_\kappa = 0.5$ (25% of metals in dust) for model "b."

The effective optical depth peaks at about $z \approx 5$ with a maximum value below $\tau^{(\mathrm{eff})} \lesssim 0.08$ for the model with the highest dust-to-gas ratio. As the emission redshift increases, the optical depth at fixed emitted wavelength decreases. In fact, despite the increase in the redshift density $n(z)$, high-z absorbers are characterized by a lower metallicity, decreasing exponentially with z in our model, while absorbers at lower z are traversed by light that has been redshifted toward progressively longer wavelengths, where the absorbers are more transparent. This explains the shape

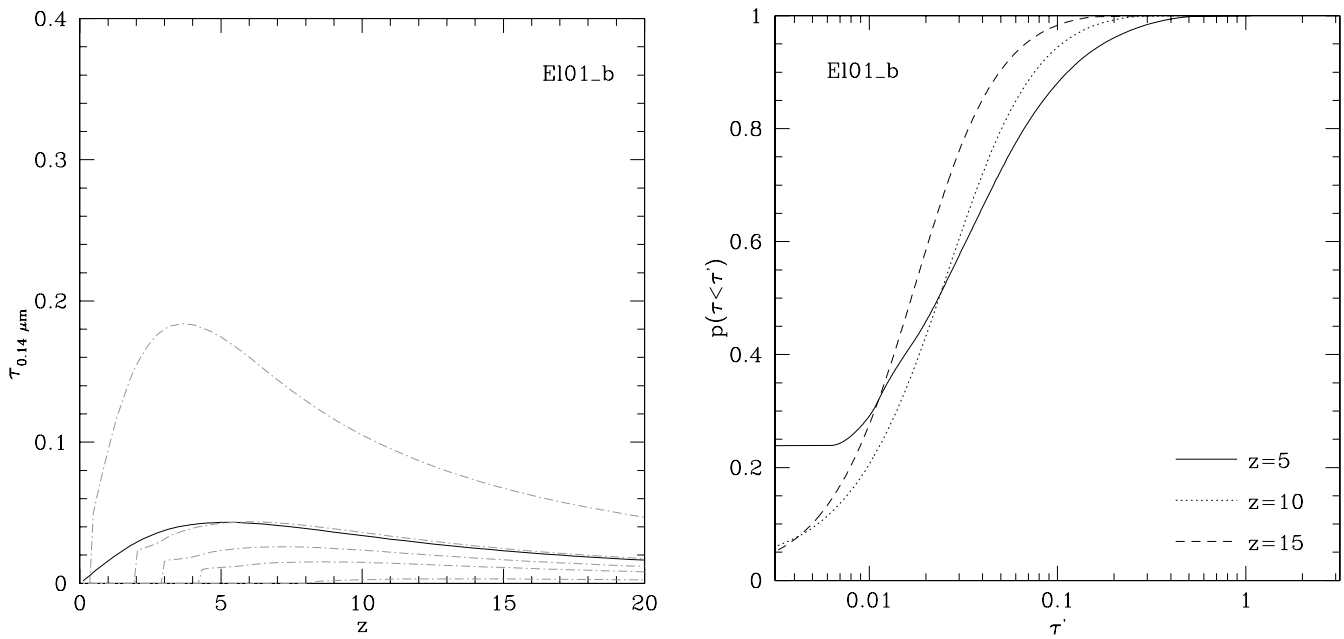

FIG. 4.—Same as Fig. 3, but for the El01_b model. [*See the electronic edition of the Journal for color version of this figure.*]

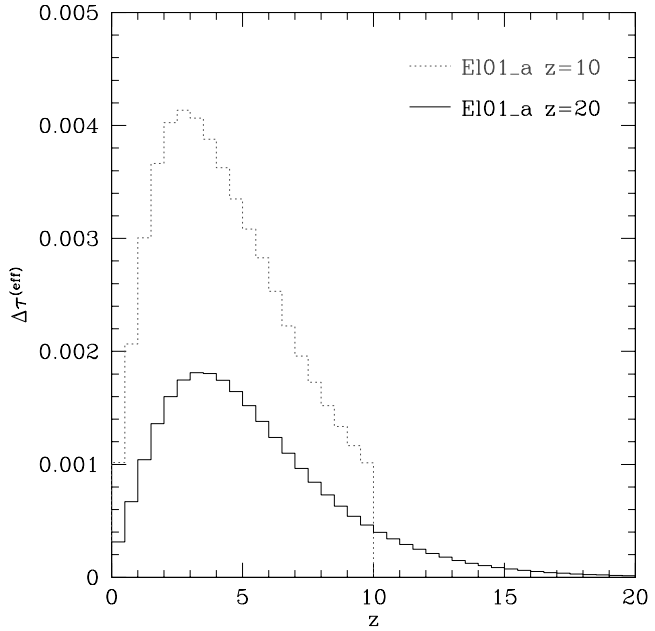

FIG. 5.—Contribution to the integral in eq. [9] divided into redshift bins. The main contribution to the effective optical depth to high-redshift sources is given by absorbers at $2 \lesssim z \lesssim 5$. [*See the electronic edition of the Journal for a color version of this figure*.]

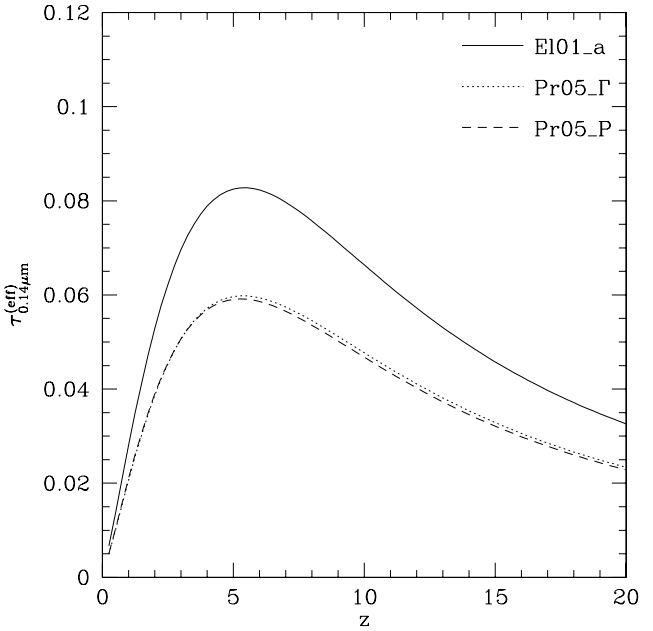

FIG. 6.—Effective optical depth at an emitted wavelength $\lambda_e = 0.14$ μm for the two Pr05 models compared with the El01_a model.

of the differential contribution to the effective optical depth shown in Figure 5. Even for $z > 10$ observations, the main contribution to absorption comes from systems at $2 \lesssim z \lesssim 5$, which is a range probed with the highest accuracy by current DLA surveys.

The optical depth distribution is characterized by a small number of highly obscured lines of sight, while the vast majority is almost dust free; e.g., for our standard model (El01_a) along a random direction, $\tau < 0.1$ with probability $\approx$0.8. Only 5% of the lines of sight may have $\tau \gtrsim 0.35$ to $z = 5$; while to $z = 20$, we have $\tau < 0.1$ with probability 0.95. In the El01_b model the optical depth is below 0.2 with probability 0.95 at $z \approx 5$ and declines below 0.1 for $z \gtrsim 12$ with probability 0.95. The optical depth distribution (Figs. 3–4) shows a sharp rise from 0 to the value of the minimum optical depth for a single absorber at the redshift where the probability of having a clear line of sight falls below the probability associated to the line plotted.

Decreasing the dust-to-gas ratio (models El01_a–El01_c) leads to a corresponding quasi-linear decrease in the effective optical depth (see eq. [9] and compare Fig. 4 [model El01_b] with Fig. 3 [model El01_a]).

Even if we consider alternative models, the expected effective optical depth does not change dramatically. In Figure 6 we report the optical depth distribution for our models calibrated to the SDSS DLA survey data. The two different models considered [Pr05_P (power law) and Pr05_Γ (gamma function) for $\Phi(N_d)$] have negligible differences between each other in terms of the resulting effective optical depth. The SDSS data suggest an effective optical depth that is about 30% smaller than that of the CORALS data.

In Figure 7 we explore the effects of variations of different assumptions for the modeling of the absorber distribution. One important parameter that is difficult to constraint observationally is the cutoff value $N_{\rm max}$ for the power-law form of $\Phi(N_d)$ used to fit the CORALS data. We have considered two additional models, El01_d and El01_e, with cutoffs 2 and 10 times higher, respectively, than El01_a (see Table 1). The effective optical depth (shown in Fig. 7) changes by $\Delta\tau^{(\rm eff)} \lesssim 0.02$, going from El01_a to El01_e. Absorbers with high dust column densities, which may have been missed in the CORALS survey due to small-number statistics (and which are likely to be missed in optically selected surveys like SDSS), have only a modest effect on the expected average transmission. One caveat is that this conclusion has been reached by extrapolating a power-law column density distribution into a region of the parameter space ($N_d > 10^{22}$ cm^{-2}) where there are no observational constraints. These systems may well be a distinct population of absorbers with column density and dust-to-gas ratio distributions different from those of the observed DLAs. In particular, an absorber with $N_d > 10^{22}$ cm^{-2} may contain H_2 and hence have a higher dust-to-gas ratio. An upper limit to the uncertainty introduced on the expected average

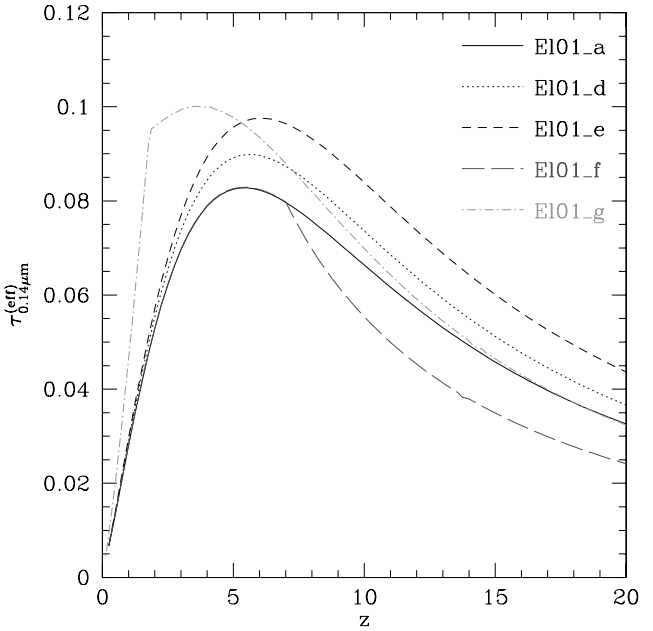

FIG. 7.—Effective optical depth at an emitted wavelength $\lambda_e = 0.14$ μm for different models. [*See the electronic edition of the Journal for a color version of this figure*.]

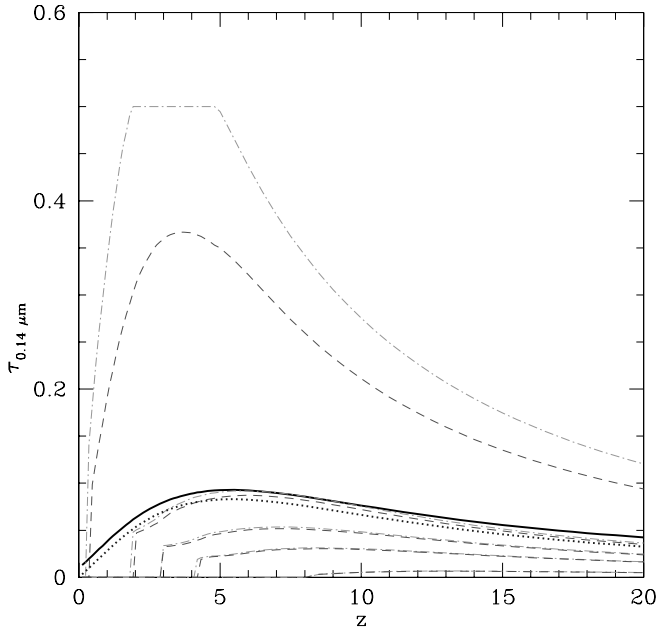

FIG. 8.—Optical depth vs. redshift for the model El01_h compared with the model El01_a. Effective optical depth is the thick black line for El01_h and the thick dotted line for El01_a. The dash-dotted lines represent for El01_h, starting from the top, the top 95% contour in the distribution of optical depth, the top 68%, the median, the bottom 32%, and the bottom 5%. The dashed lines represent the same quantities, but for El01_a. [*See the electronic edition of the Journal for a color version of this figure*.]

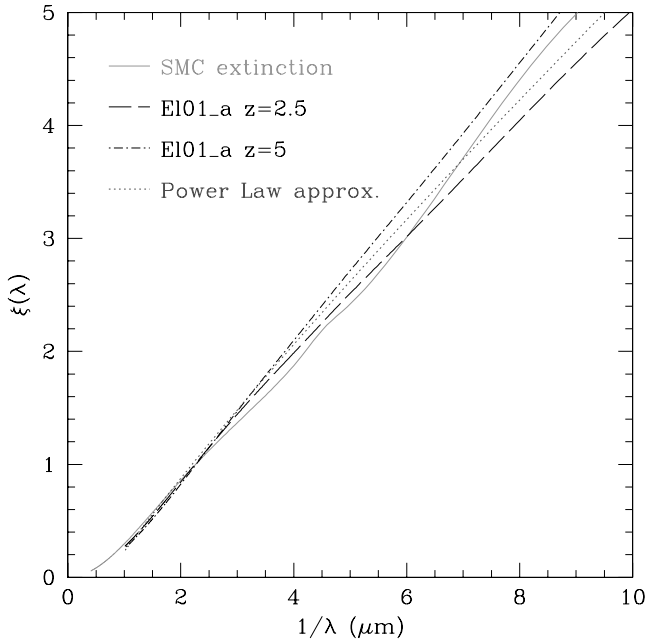

FIG. 9.—Effective mean extinction curve $\langle \xi(\lambda) \rangle = \ln(E[q(\lambda)]/\ln(E[q(\lambda_B)]))$ for the El01_a model at $z = 2.5$ (*dashed line*) and $z = 5$, (*dot-dashed line*) compared with the input SMC extinction curve (*solid line*). Our analytical fitting formula, eq. (17) (*dotted line*), is shown for comparison. [*See the electronic edition of the Journal for a color version of this figure*.]

transmission by a hypothetical population of "bricks" absorbers can be estimated from the CORALS survey. At the 95% confidence level this population influences less than 2.9% of the lines of sight. At this confidence level the maximum displacement introduced in $\tau^{(\mathrm{eff})}$ is $\Delta\tau^{(\mathrm{eff})} \lesssim 0.03$, in good agreement with the estimate $\Delta\tau^{(\mathrm{eff})} \lesssim 0.02$ that we obtain with our El01_e model (for the effects of dust-rich absorbers, see also model El01_h discussed below).

Model El01_f (shown in Fig. 7) is characterized by a cutoff of the absorbers distribution at $z = 7$, while otherwise it coincides with the model El01_a. This allows us to quantify the uncertainties associated with the extrapolation of our models to redshifts where DLA data are unavailable. The possibility that the DLA number density may drop significantly at high redshift is hinted at by semianalytical models (Johansson & Efstathiou 2006). Even in the extreme scenario of model El01_f, where the DLA number is set to 0 for $z > 7$, the difference in the average effective optical depth is only $\Delta\tau^{(\mathrm{eff})} \lesssim 0.008$.

Model El01_g investigates the effects of the presence of a subpopulation of DLA systems at $z \lesssim 1.8$ with high metallicity (Wild & Hewett 2005; Wild et al. 2006). This model has been constructed starting from the standard El01_a and assuming that one-third of the DLA systems at $z < 1.8$ have solar metallicity. The presence of a significant number of these systems at higher z is unlikely, as the metallicity in the CORALS survey is significantly subsolar and consistent with that measured in optically selected surveys (Akerman et al. 2005). The effect of this population of absorbers is to enhance the optical depth up to $z \lesssim 6$ (see Fig. 7). However, as the emission redshift further increases, their influence is significantly reduced and becomes negligible for $z \gtrsim 10$.

Model El01_h continues to investigate the effects of a small population of optically thick absorbers (like the inner regions of spiral galaxies or dusty starbust galaxies like M82) that could have been missed in the CORALS survey due to the limited number of lines of sight probed. We assume that a random line of sight intersects a number of galaxies drawn from a Poisson distribution with average 0.025.[1]

We assume that each galaxy introduces an optical depth of 0.5 (estimated from Holwerda et al. [2005]). The results of the Monte Carlo simulation (shown in Fig. 8) indicate that the effective optical depth is slightly higher in this case (i.e., the average transmission is marginally lower with respect to El01_a). At the level of the optical depth distribution, only the contour lines associated with transmission $\ll 1$ are influenced, i.e., those directly affected by lines of sight intersecting a galaxy. Differences between the El01_h and the El01_a models appear significant only for the top 10% of the distribution.

5.1. *Reddening*

The shape of the effective extinction curve $E[\xi(\lambda)] \equiv \log E[q(\lambda, z_e)]/\log E[q(\lambda_B, z_e)]$ is only marginally dependent on the model used or on the emission redshift considered (see Fig. 9). We can empirically fit in the range $\lambda_e \in [0.1\ \mu\mathrm{m},\ 8\ \mu\mathrm{m}]$ the effective average extinction curve for emitters at redshift $z \gtrsim 1$ with a simple power law in the form

$$E[\xi(\lambda_e)] = \eta - \left(\frac{\kappa}{\lambda_e}\right)^{\zeta}, \tag{17}$$

[1] This value for the covering factor has been estimated as sum of two contributions at high and low redshift. For the high-redshift contribution we have analyzed the Hubble Ultra Deep Field. In the i_{775} band the covering factor of pixels brighter than $m_i = 33$ is $\approx$0.01. This number is broadly compatible with what is derived from the luminosity function of Lyman break galaxies in the redshift range $2 \leq z \leq 6$ (Steidel et al. 1999; Ferguson et al. 2004; Bouwens et al. 2006) and extrapolated down to $z = 1$. To estimate the covering factor due to galaxies at $z < 1$, we have considered four SDSS random fields in the i band for a total area of $\approx$0.15 deg^2. For each field we have applied a cut at +2.5 σ from the sky level and then removed isolated pixels. This analysis provides an estimate of the covering factor of $\approx$0.015, with single field values in the range [0.008, 0.022].

with $\eta = -0.55$, $\kappa = 0.755$ μm, and $\zeta = 0.87$. With this "universal" extinction curve, we can infer the typical values for the average reddening, e.g., $E(B-V)$, which can be estimated as a fixed fraction of the effective optical depth $\tau^{(\mathrm{eff})}$ at a reference wavelength.

6. DISCUSSION

We present a model for quantifying the effects of absorption due to dust in DLA systems along the line of sight for sources up to $z = 20$. The effective optical depth to a given redshift as a function of the emitted frequency λ_e can be evaluated analytically by using eq. [9]. This allows one to obtain immediately an order-of-magnitude estimate of the effects of the dust absorption on the average transmission for the class of observations one is interested in.

For a better characterization of the effects of the extinction, we study by means of a Monte Carlo method the distribution of the optical depths to a given redshift, setting upper and lower limits on the dust extinction. Under the reference scenario, which accounts for a large fraction of metals in dust grains (model El01_a with 50% of the metals in dust), the effects of dust obscuration remain modest even for very high redshift, with an optical depth at $\lambda_e = 0.14$ μm below 0.4 with probability 0.95 for $z_e \approx 3$. As the emission redshift increases, the optical depth decreases, and for $z_e \gtrsim 15$ our modeling predicts $\tau \lesssim 0.1$ with probability 0.95. We have explored several alternative possibilities for the input parameters, finding that the effective optical depth varies within a factor 2 at most, even when a population of optically thick absorbers like the central parts of star-forming galaxies is taken into account. Therefore, the loss of sensitivity and the effects of reddening are not expected to significantly influence high-z observations with the *James Webb Space Telescope* (*JWST*).

In the future we plan to extend the present framework to include additional effects on the transmission along the line of sight, such as gravitational lensing magnification and demagnification, which may be significant for explaining the observed number counts of bright quasars in the SDSS DLA survey (Prochaska et al. 2005).

It is our pleasure to thank Mike Fall, Harry Ferguson, Benne Holwerda, and Jason Xavier Prochaska for interesting discussions and valuable comments. We also thank Peter Johansson for providing additional unpublished data from his semianalytical model for formation and evolution of DLA systems. We are grateful to the referee for constructive suggestions that have improved the paper. This work was supported in part by NASA *JWST* IDS grant NAG 5-12458.

REFERENCES

Akerman, C. J., Ellison, S. L., Pettini, M., & Steidel, C. C. 2005, A&A, 440, 449
Bouwens, R. J., Illingworth, G. D., Blakeslee, J. P., & Franx, M. 2006, ApJ, in press (astro-ph/0509641)
Calzetti, D., Kinney, A. L., & Storchi-Bergmann, T. 1994, ApJ, 429, 582
Cen, R., Ostriker, J. P., Prochaska, J. X., & Wolfe, A. M. 2003, ApJ, 598, 741
Ellison, S. L., Hall, P. B., & Lira, P. 2005, AJ, 130, 1345
Ellison, S. L., Yan, L., Hook, I. M., Wall, J. V., & Shaver, P. 2001, A&A, 379, 393
Fall, S. M., & Pei, Y. C. 1989, ApJ, 337, 7
———. 1993, ApJ, 402, 479
Ferguson, H. C., et al. 2004, ApJ, 600, 107
Holwerda, B. W., González, R. A., van der Kruit, P. C., & Allen, R. J. 2005, AJ, 129, 1396
Johansson, P. H., & Efstathiou, G. 2006, MNRAS, 371, 1519
Junkkarinen, V. T., Cohen, R. D., Beaver, E. A., Burbidge, E. M., Lyons, R. W., & Madejski, G. 2004, ApJ, 614, 658
Kulkarni, V. P., Fall, S. M., Lauroesch, J. T., York, D. G., Welty, D. E., Khare, P., & Truran, J. W. 2005, ApJ, 618, 68
Madau, P. 1995, ApJ, 441, 18
Møller, P., & Jackobsen, P. 1990, A&A, 228, 299
Murphy, M. T., & Liske, J. 2004, MNRAS, 354, L31
Ostriker, J. P., & Heisler, J. 1984, ApJ, 278, 1
Papovich, C., Dickinson, M., & Ferguson, H. C. 2001, ApJ, 559, 620
Pei, Y. C. 1992, ApJ, 395, 130
Pei, Y. C., & Fall, S. M. 1995, ApJ, 454, 69
Pei, Y. C., Fall, S. M., & Bechtold, J. 1991, ApJ, 378, 6
Pei, Y. C., Fall, S. M., & Hauser, M. G. 1999, ApJ, 522, 604
Pettini, M., King, D. L., Smith, L. J., & Hunstead, R. W. 1997, ApJ, 478, 536
Press, W. H., Teukolsky, S. A., Vetterling, W. T., & Flannery, B. P. 1992, Numerical Recipes in Fortran 77: The Art of Scientific Computing (2nd ed.; Cambridge: Cambridge Univ. Press)
Prochaska, J. X., Gawiser, E., Wolfe, A. M., Cooke, J., & Gelino, D. 2003, ApJS, 147, 227
Prochaska, J. X., Herbert-Fort, S., & Wolfe, A. M. 2005, ApJ, 635, 123
Prochaska, J. X., & Wolfe, A. M. 2002, ApJ, 566, 68
Rao, S. M., Turnshek, D. A., & Nestor, D. B. 2006, ApJ, 636, 610
Spergel, D. N., et al. 2006, ApJ, submitted (astro-ph/0603449)
Steidel, C. C., Adelberger, K. L., Giavalisco, M., Dickinson, M., & Pettini, M. 1999, ApJ, 519, 1
Stiavelli, M., Fall, S. M., & Panagia, N. 2004, ApJ, 600, 508
Trenti, M., & Stiavelli, M. 2006, ApJ, 651, 51
Wild, V., & Hewett, P. C. 2005, MNRAS, 361, L30
Wild, V., Hewett, P. C., & Pettini, M. 2006, MNRAS, 367, 211
Wolfe, A. M., Gawiser, E., & Prochaska, J. X. 2005, ARA&A, 43, 861
York, D. G., et al. 2006, MNRAS, 367, 945